Helsinki University of Technology, Institute of Mathematics, Research Reports
Teknillisen korkeakoulun matematiikan laitoksen tutkimusraporttisarja
Espoo 2005 A474

SUPERCONVERGENCE AND POSTPROCESSING OF MITC PLATE ELEMENTS

Mikko Lyly Jarkko Niiranen Rolf Stenberg

TEKNILLINEN KORKEAKOULU
TEKNISKA HÖGSKOLAN
HELSINKI UNIVERSITY OF TECHNOLOGY
TECHNISCHE UNIVERSITÄT HELSINKI
UNIVERSITE DE TECHNOLOGIE D'HELSINKI

Helsinki University of Technology, Institute of Mathematics, Research Reports
Teknillisen korkeakoulun matematiikan laitoksen tutkimusraporttisarja
Espoo 2005 A474

SUPERCONVERGENCE AND POSTPROCESSING OF MITC PLATE ELEMENTS

Mikko Lyly **Jarkko Niiranen** **Rolf Stenberg**

Helsinki University of Technology
Department of Engineering Physics and Mathematics
Institute of Mathematics

Mikko Lyly, Jarkko Niiranen, Rolf Stenberg: *Superconvergence and postprocessing of MITC plate elements*; Helsinki University of Technology, Institute of Mathematics, Research Reports A474 (2005).

Abstract: *In this paper the MITC finite element methods for the Reissner–Mindlin plate bending problem are considered. A superconvergence result for the deflection is proved. Utilizing this property a local postprocessing is introduced and analyzed. The improved accuracy of the deflection is confirmed by numerical computations.*

AMS subject classifications: 65N30, 74S05, 74K20

Keywords: Reissner–Mindlin plates, MITC finite element methods, superconvergence, postprocessing

Correspondence

Mikko.Lyly@csc.fi, Jarkko.Niiranen@tkk.fi, Rolf.Stenberg@tkk.fi

ISBN 951-22-7310-1
ISSN 0784-3143

Helsinki University of Technology
Department of Engineering Physics and Mathematics
Institute of Mathematics
P.O. Box 1100, 02015 HUT, Finland
email:math@hut.fi http://www.math.hut.fi/

1 Introduction

The main difficulty with the design and analysis of the finite element methods for the Reissner–Mindlin plate model is the locking phenomena. This can be understood as an incorrect numerical capturing of the plate asymptotics. In the limit when the plate thickness approaches zero, the Reissner–Mindlin model approaches the Kirchhoff model for which the vertical deflection w and the rotation $\boldsymbol{\beta}$ satisfy the constraint

$$\nabla w - \boldsymbol{\beta} = \mathbf{0}. \tag{1.1}$$

In the basic finite element method the exact fulfilment of (1.1) for the discrete solution $(w_h, \boldsymbol{\beta}_h)$ leads to the locking. In the MITC elements this is overcome by introducing a reduction operator $\boldsymbol{R}_h$ on the shear deformation and in the limit the discrete constraint is

$$\boldsymbol{R}_h(\nabla w_h - \boldsymbol{\beta}_h) = \mathbf{0}. \tag{1.2}$$

In order that the method is stable the rotation has also to be augmented by bubble degrees of freedom. Otherwise, equal order basis functions for both the deflection and the rotation are used. That this can be done with an optimal order of convergence might look surprising as in the limit the rotation is the gradient of the deflection.

The purpose of this paper is to show that since the optimal order of convergence is obtained for equal order approximation the approximate solution contains sufficient information so that one can, by an element by element postprocessing, construct an new approximation for the deflection which is a piecewise polynomial one degree higher than the original one and with an improved convergence rate. For the construction of the postprocessing a superconvergence result of the original method is used. A part of this result is, roughly speaking, that the vertex values obtained with the MITC methods are superconvergent. (This may also be an explanation why these methods have become so popular.)

The plan of this paper is the following. In the next two sections the Reissner–Mindlin plate model and the MITC methods are recalled. Then, in Sections 4 and 5, the superconvergence result is proved and the postprocessing is introduced for which the improved estimate is derived. In Section 6 the postprocessing is verified by benchmark computations.

In the paper we use standard notation in connection with finite element methods.

2 The Reissner–Mindlin plate model

We consider a linearly elastic and isotropic plate with the shear modulus G and the Poisson ratio ν. The midsurface of the undeformed plate is $\Omega \subset \mathbb{R}^2$ and the plate thickness is constant and denoted by t.

It is supposed that the boundary of the plate is divided into hard clamped, hard simply supported and free parts: $\partial\Omega = \Gamma_{\mathrm{C}} \cup \Gamma_{\mathrm{SS}} \cup \Gamma_{\mathrm{F}}$. (The soft clamped and soft simply supported cases would be possible as well.) The spaces of kinematically admissible deflections and rotations are then

$$W = \{v \in H^1(\Omega) \mid v_{|\Gamma_{\mathrm{C}}} = 0,\ v_{|\Gamma_{\mathrm{SS}}} = 0\} \tag{2.1}$$

and

$$\boldsymbol{V} = \{\boldsymbol{\eta} \in [H^1(\Omega)]^2 \mid \boldsymbol{\eta}_{|\Gamma_{\mathrm{C}}} = \boldsymbol{0},\ (\boldsymbol{\eta} \cdot \boldsymbol{\tau})_{|\Gamma_{\mathrm{SS}}} = 0\}. \tag{2.2}$$

where $\boldsymbol{\tau}$ is the unit tangent to the boundary. We define the following bilinear form

$$\mathcal{B}(z, \boldsymbol{\phi}; v, \boldsymbol{\eta}) = a(\boldsymbol{\phi}, \boldsymbol{\eta}) + t^{-2}(\nabla z - \boldsymbol{\phi}, \nabla v - \boldsymbol{\eta}), \tag{2.3}$$

with

$$a(\boldsymbol{\phi}, \boldsymbol{\eta}) = \frac{1}{6}\{(\boldsymbol{\varepsilon}(\boldsymbol{\phi}), \boldsymbol{\varepsilon}(\boldsymbol{\eta})) + \frac{\nu}{1-\nu}(\operatorname{div} \boldsymbol{\phi}, \operatorname{div} \boldsymbol{\eta})\}, \tag{2.4}$$

where the linear strain tensor is

$$\boldsymbol{\varepsilon}(\boldsymbol{\eta}) = \frac{1}{2}(\nabla \boldsymbol{\eta} + (\nabla \boldsymbol{\eta})^T). \tag{2.5}$$

The transverse loading f we assume to be given as $f = Gt^3 g$, where $g \in H^{-1}(\Omega)$ is independent of t. This is done in order to get a non-trivial solution to the problem in the limit $t \to 0$ (i.e. to the Kirchhoff–Love model) [11], [5, Theorem 3.1, p. 300].

With these assumptions and notation the variational formulation for the Reissner–Mindlin plate model can be written in the following form [5], [11]:

Variational formulation 2.1. *Find the deflection $w \in W$ and the rotation $\boldsymbol{\beta} \in \boldsymbol{V}$ such that*

$$\mathcal{B}(w, \boldsymbol{\beta}; v, \boldsymbol{\eta}) = (g, v) \ \ \forall (v, \boldsymbol{\eta}) \in W \times \boldsymbol{V}. \tag{2.6}$$

For the analysis we will also need to write the problem in mixed form in which the shear force

$$\boldsymbol{q} = \frac{1}{t^2}(\nabla w - \boldsymbol{\beta}) \tag{2.7}$$

is taken as an independent unknown in the space $\boldsymbol{Q} = [L^2(\Omega)]^2$ (cf. [5] and [11]) and we get the

Variational formulation 2.2. *Find $(w, \boldsymbol{\beta}, \boldsymbol{q}) \in W \times \boldsymbol{V} \times \boldsymbol{Q}$ such that*

$$a(\boldsymbol{\beta}, \boldsymbol{\eta}) + (\boldsymbol{q}, \nabla v - \boldsymbol{\eta}) = (g, v) \ \ \forall (v, \boldsymbol{\eta}) \in W \times \boldsymbol{V}, \tag{2.8}$$

$$(\nabla w - \boldsymbol{\beta}, \boldsymbol{r}) - t^2(\boldsymbol{q}, \boldsymbol{r}) = 0 \ \ \forall \boldsymbol{r} \in \boldsymbol{Q}. \tag{2.9}$$

3 The MITC Finite Elements

In this section we will recall the so called MITC plate bending elements [4, 5, 6]. For simplicity we consider the triangular family but we emphasize that all the results are valid for quadrilateral families as well. By $\mathcal{C}_h$ we denote the triangulation of $\overline{\Omega}$. As usual we denote $h = \max_{K\in\mathcal{C}_h} h_K$, where h_K is the diameter of K. The space of polynomials of degree k on K is denoted by $P_k(K)$. By C and C_i we denote positive constants independent of the thickness t and the mesh size h.

In the MITC method the finite element subspaces $W_h \subset W$ and $\boldsymbol{V}_h \subset \boldsymbol{V}$ are defined for the polynomial degree $k \geq 2$ as follows

$$W_h = \{w \in W \mid w_{|K} \in P_k(K) \ \ \forall K \in \mathcal{C}_h\}, \tag{3.1}$$
$$\boldsymbol{V}_h = \{\boldsymbol{\eta} \in \boldsymbol{V} \mid \boldsymbol{\eta}_{|K} \in [P_k(K)]^2 \oplus [B_{k+1}(K)]^2 \ \ \forall K \in \mathcal{C}_h\}, \tag{3.2}$$

with the "bubble space"

$$B_{k+1}(K) = \{b = b_3 p \mid p \in \tilde{P}_{k-2}(K),\ b_3 \in P_3(K),\ b_{3|E} = 0 \ \ \forall E \subset \partial K\}, \tag{3.3}$$

where $\widetilde{P}_{k-2}(K)$ is the space of homogeneous polynomials of degree $k-2$ on the element K.

We denote the rotated Raviart–Thomas space of order $k-1$ by

$$\boldsymbol{Q}_h = \{\, \boldsymbol{r} \in \boldsymbol{H}(\mathrm{rot} : \Omega) \mid \boldsymbol{r}_{|K} \in [P_{k-1}(K)]^2 \oplus (y, -x)\tilde{P}_{k-1}(K) \ \forall K \in \mathcal{C}_h \,\}. \tag{3.4}$$

Note that the requirement $\boldsymbol{Q}_h \subset \boldsymbol{H}(\mathrm{rot} : \Omega)$ implies that the tangential components of functions in $\boldsymbol{Q}_h$ are continuous along inter element boundaries. Next, we define the reduction operator $\boldsymbol{R}_h : [H^1(\Omega)]^2 \to \boldsymbol{Q}_h$ through the conditions, with $\boldsymbol{R}_K = \boldsymbol{R}_{h|K}$,

$$\begin{aligned} \langle (\boldsymbol{R}_K\boldsymbol{\eta} - \boldsymbol{\eta}) \cdot \boldsymbol{\tau}_E, p\rangle_E = 0 \ \ \forall p \in P_{k-1}(E) \ \ \forall E \subset \partial K, \\ (\boldsymbol{R}_K\boldsymbol{\eta} - \boldsymbol{\eta}, \boldsymbol{p})_K = 0 \ \ \forall \boldsymbol{p} \in [P_{k-2}(K)]^2, \end{aligned} \tag{3.5}$$

where E denotes an edge to K and $\boldsymbol{\tau}_E$ is the unit tangent to E. $(\cdot,\cdot)_K$ and $\langle\cdot,\cdot\rangle_E$ are the L^2 inner products.

The method is now defined as

Method 3.1. *Find the deflection $w_h \in W_h$ and the rotation $\boldsymbol{\beta}_h \in \boldsymbol{V}_h$ such that*

$$\mathcal{B}_h(w_h, \boldsymbol{\beta}_h; v, \boldsymbol{\eta}) = (g, v) \ \ \forall (v, \boldsymbol{\eta}) \in W_h \times \boldsymbol{V}_h, \tag{3.6}$$

with the modified bilinear form

$$\mathcal{B}_h(z, \boldsymbol{\phi}; v, \boldsymbol{\eta}) = a(\boldsymbol{\phi}, \boldsymbol{\eta}) + \frac{1}{t^2}(\boldsymbol{R}_h(\nabla z - \boldsymbol{\phi}), \boldsymbol{R}_h(\nabla v - \boldsymbol{\eta})). \tag{3.7}$$

The discrete shear force $\boldsymbol{q}_h \in \boldsymbol{Q}_h$ is

$$\boldsymbol{q}_h = \frac{1}{t^2}\boldsymbol{R}_h(\nabla w_h - \boldsymbol{\beta}_h). \tag{3.8}$$

Now, the mixed variant of Method 3.1 is of the following form [6]:

Method 3.2. *Find* $(w_h, \boldsymbol{\beta}_h, \boldsymbol{q}_h) \in W_h \times \boldsymbol{V}_h \times \boldsymbol{Q}_h \subset W \times \boldsymbol{V} \times \boldsymbol{Q}$ *such that*

$$a(\boldsymbol{\beta}_h, \boldsymbol{\eta}) + (\boldsymbol{q}_h, \boldsymbol{R}_h(\nabla v - \boldsymbol{\eta})) = (g, v) \ \ \forall (v, \boldsymbol{\eta}) \in W_h \times \boldsymbol{V}_h, \tag{3.9}$$

$$(\boldsymbol{R}_h(\nabla w_h - \boldsymbol{\beta}_h), \boldsymbol{r}) - t^2(\boldsymbol{q}_h, \boldsymbol{r}) = 0 \ \ \forall \boldsymbol{r} \in \boldsymbol{Q}_h. \tag{3.10}$$

An error analysis of the method has been performed in [6, 10]. In these works the estimates were given assuming a smooth solution. This assumption is, however, unrealistic since in general the solution has boundary layers, cf. [2] and [3]. For a polygonal domain the solution also contains corner singularities and a complete characterization of the behavior of the solution does not seem to be available.

The only error analyses known to us in which the boundary layers are taken into account are references [12, 7]. In these works the case of a free boundary is considered. It is shown that due to the strong boundary layer the error contains a term which is of the order $\mathcal{O}(h^{1/2})$.

In [9] we have performed a refined error analysis, in the spirit of [12], for the clamped plate and a convex domain. We first prove the following regularity estimate. Here, we write $w = w_0 + w_r$, where w_0 is the deflection for the limiting Kirchhoff problem. By $\Omega_i \subset\subset \Omega$ we denote a region compactly embedded in Ω.

Theorem 3.1. *Let* $\Omega \subset \mathbb{R}^2$ *be a convex polygon and* $\Omega_i \subset\subset \Omega$. *Let* $(w, \boldsymbol{\beta}, \boldsymbol{q})$ *be the solution to problem 2.2 with clamped boundaries and let* $w = w_0 + w_r$, *where* w_0 *is the solution in the limit* $t \to 0$. *Then with* $g \in H^{s-2}(\Omega)$ *and* $tg \in H^{s-1}(\Omega)$, $s \geq 1$,

$$\|w_0\|_3 + \frac{1}{t}\|w_r\|_2 + \|\boldsymbol{\beta}\|_2 + \|\boldsymbol{q}\|_0 + t\|\boldsymbol{q}\|_1 \leq C(\|g\|_{-1} + t\|g\|_0), \tag{3.11}$$

$$\begin{aligned} &\|w_0\|_{s+2,\Omega_i} + \frac{1}{t}\|w_r\|_{s+1,\Omega_i} + \|\boldsymbol{\beta}\|_{s+1,\Omega_i} + \|\boldsymbol{q}\|_{s-1,\Omega_i} + t\|\boldsymbol{q}\|_{s,\Omega_i} \\ &\leq C(\|g\|_{s-2} + t\|g\|_{s-1}). \end{aligned} \tag{3.12}$$

When denoting the mesh size in the interior by $h_i = \max_{K \subset \Omega_i} h_K$ and near the boundary by $h_b = \max_{K \not\subset \Omega_i} h_K$ we can state the error estimate as follows [9].

Theorem 3.2. *Let* Ω *be a convex polygon and suppose that the plate is clamped. For* $g \in H^{k-2}(\Omega)$, $tg \in H^{k-1}(\Omega)$ *it then holds*

$$\begin{aligned} &\|w - w_h\|_1 + \|\boldsymbol{\beta} - \boldsymbol{\beta}_h\|_1 + t\|\boldsymbol{q} - \boldsymbol{q}_h\|_0 + \|\boldsymbol{q} - \boldsymbol{q}_h\|_{-1} \\ &\quad \leq C\{h_i^k(\|g\|_{k-2} + t\|g\|_{k-1}) + h_b(\|g\|_{-1} + t\|g\|_0)\} \end{aligned} \tag{3.13}$$

and

$$\begin{aligned} &\|w - w_h\|_0 + \|\boldsymbol{\beta} - \boldsymbol{\beta}_h\|_0 \\ &\leq Ch\{h_i^k(\|g\|_{k-2} + t\|g\|_{k-1}) + h_b(\|g\|_{-1} + t\|g\|_0)\}. \end{aligned} \tag{3.14}$$

4 Superconvergence of the deflection

In this section we prove a superconvergence result for the deflection. For this we need a classical interpolation operator (cf. [8, Lemmas A.3, A.4, p. 100, 101]) that we now recall.

Definition 4.1. Let a and E be a vertex and an edge of the triangle K. The interpolation operator $I_h : H^s(\Omega) \to W_h$, $s > 1$, is defined through the conditions

$$\begin{aligned} &(v - I_K v)(a) = 0 \ \ \forall a \in K, \\ &\langle v - I_K v, p\rangle_E = 0 \ \ \forall p \in P_{k-2}(E) \ \ \forall E \subset K, \\ &(v - I_K v, p)_K = 0 \ \ \forall p \in P_{k-3}(K), \end{aligned} \tag{4.1}$$

for $I_K = I_{h|K} \ \ \forall K \in \mathcal{C}_h$.

The interpolation operator is quasi-optimal [8].

Lemma 4.1. *There exists a constant $C > 0$ such that*

$$\|I_K v - v\|_{1,K} \le C h_K^{m-1} \|v\|_{m,K} \ \ \forall v \in H^m(K), \tag{4.2}$$

where $2 \le m \le k+1$.

This interpolation estimate gives the following result.

Lemma 4.2. *There is a positive constant C such that*

$$\|w - I_h w\|_1 \le C\{h_i^k(\|g\|_{k-2} + t\|g\|_{k-1}) + h_b(\|g\|_{-1} + t\|g\|_0)\}. \tag{4.3}$$

Proof. Applying the above result with $m = k+1$ for $K \subset \Omega_i$ and $m = 2$ for $K \subset \Omega_b$ gives

$$\begin{aligned} \|w - I_h w\|_1 &\le \|w - I_h w\|_{1,\Omega_i} + \|w - I_h w\|_{1,\Omega_b} \\ &\le C\big(h_i^k \|w\|_{k+1,\Omega_i} + h_b \|w\|_{2,\Omega_b}\big). \end{aligned} \tag{4.4}$$

Theorem 3.1 gives

$$\|w\|_{k+1,\Omega_i} \le C(\|g\|_{k-2} + t\|g\|_{k-1}) \tag{4.5}$$

and

$$\|w\|_2 \le C(\|g\|_{-1} + t\|g\|_0), \tag{4.6}$$

which proves the asserted estimate. □

For the proof of the superconvergence result we further need the following approximation property of the reduction operator.

Lemma 4.3. [13] *There is a positive constant $C > 0$ such that*

$$\|\boldsymbol{\eta} - \boldsymbol{R}_K \boldsymbol{\eta}\|_{0,K} \le C h_K^m \|\boldsymbol{\eta}\|_{m,K} \ \ \forall \boldsymbol{\eta} \in [H^m(K)]^2, \tag{4.7}$$

where $1 \le m \le k$.

From this we get the following estimate.

Lemma 4.4. *There is a positive constant C such that*

$$t\|\boldsymbol{q} - \boldsymbol{R}_h\boldsymbol{q}\|_0 \leq C\{h_i^k(\|g\|_{k-2} + t\|g\|_{k-1}) + h_b(\|g\|_{-1} + t\|g\|_0)\}. \tag{4.8}$$

Proof. We use the previous estimate with $m = k$ and $m = 1$:

$$\|\boldsymbol{q} - \boldsymbol{R}_h\boldsymbol{q}\|_0 \leq \|\boldsymbol{q} - \boldsymbol{R}_h\boldsymbol{q}\|_{0,\Omega_i} + \|\boldsymbol{q} - \boldsymbol{R}_h\boldsymbol{q}\|_{0,\Omega_b} \tag{4.9}$$

$$\leq C\big(h_i^k\|\boldsymbol{q}\|_{k,\Omega_i} + h_b\|\boldsymbol{q}\|_{1,\Omega_b}\big). \tag{4.10}$$

By Theorem 3.1 we get

$$t\|\boldsymbol{q}\|_{k,\Omega_i} \leq C(\|g\|_{k-2} + t\|g\|_{k-1}) \tag{4.11}$$

$$t\|\boldsymbol{q}\|_1 \leq C(\|g\|_{-1} + t\|g\|_0), \tag{4.12}$$

and the assertion is proved. □

Next we show that there is a close connection between the interpolation and reduction operators.

Lemma 4.5. *It holds*

$$\boldsymbol{R}_h\nabla v = \nabla I_h v \ \ \forall v \in H^s(\Omega),\ s \geq 2. \tag{4.13}$$

Proof. Using the first two conditions of (4.1) we have

$$\langle(\nabla I_K v - \nabla v)\cdot\boldsymbol{\tau}_E, p\rangle_E = \int_E \frac{\partial(I_K v - v)}{\partial\boldsymbol{\tau}_E}\, p \tag{4.14}$$

$$= \Big|_{\partial E}(I_K v - v)\, p - \int_E (I_K v - v)\,\frac{\partial p}{\partial\boldsymbol{\tau}_E} = 0 \ \ \forall p \in P_{k-1}(E).$$

Using the second and the third condition of (4.1) we get

$$(\nabla I_K v - \nabla v, \boldsymbol{p})_K = -(I_K v - v, \operatorname{div}\boldsymbol{p})_K = 0 \ \ \forall \boldsymbol{p} \in [P_{k-2}(K)]^2. \tag{4.15}$$

Hence, $\nabla I_K v$ fulfills the conditions (3.5) for $\boldsymbol{R}_K\nabla v$. Since $\nabla I_K v \subset \boldsymbol{Q}_{h|K}$ and the reduction operator $\boldsymbol{R}_K$ is uniquely defined, the assertion is proved. □

We now have the following result.

Theorem 4.1. *It holds*

$$\begin{aligned}\|\nabla(I_h w - w_h)\|_{0,K} \leq\ & Ch_K\|\boldsymbol{\beta} - \boldsymbol{\beta}_h\|_{1,K} + \|\boldsymbol{\beta} - \boldsymbol{\beta}_h\|_{0,K} \\ & + t^2\|\boldsymbol{q} - \boldsymbol{q}_h\|_{0,K} + t^2\|\boldsymbol{q} - \boldsymbol{R}_h\boldsymbol{q}\|_{0,K}.\end{aligned} \tag{4.16}$$

Proof. Denote $v = I_h w - w_h \in W_h$. Using Lemma 4.5, the equations (2.7), (3.8) for $\boldsymbol{q}$ and $\boldsymbol{q}_h$, respectively, we get

$$\begin{aligned}
&\|\nabla(I_h w - w_h)\|_{0,K}^2 \\
&\quad = (\nabla(I_h w - w_h), \nabla v)_K \\
&\quad = (\boldsymbol{R}_h \nabla w - \nabla w_h, \nabla v)_K \\
&\quad = (\boldsymbol{R}_h(t^2\boldsymbol{q} + \boldsymbol{\beta}) - (t^2\boldsymbol{q}_h + \boldsymbol{R}_h\boldsymbol{\beta}_h), \nabla v)_K \\
&\quad = (t^2\boldsymbol{R}_h(\boldsymbol{q} - \boldsymbol{q}_h) + \boldsymbol{R}_h(\boldsymbol{\beta} - \boldsymbol{\beta}_h), \nabla v)_K \\
&\quad \le \big(t^2\|\boldsymbol{R}_h\boldsymbol{q} - \boldsymbol{q}_h\|_{0,K} + \|\boldsymbol{R}_h(\boldsymbol{\beta} - \boldsymbol{\beta}_h)\|_{0,K}\big)\|\nabla v\|_{0,K}.
\end{aligned} \tag{4.17}$$

By the triangle inequality we have

$$\|\boldsymbol{R}_h\boldsymbol{q} - \boldsymbol{q}_h\|_{0,K} \le \|\boldsymbol{q} - \boldsymbol{q}_h\|_{0,K} + \|\boldsymbol{q} - \boldsymbol{R}_h\boldsymbol{q}\|_{0,K}. \tag{4.18}$$

Lemma 4.3 gives

$$\begin{aligned}
\|\boldsymbol{R}_h(\boldsymbol{\beta} - \boldsymbol{\beta}_h)\|_{0,K} &\le \|(\boldsymbol{R}_h - \boldsymbol{I})(\boldsymbol{\beta} - \boldsymbol{\beta}_h)\|_{0,K} + \|\boldsymbol{\beta} - \boldsymbol{\beta}_h\|_{0,K} \\
&\le Ch_K\|\boldsymbol{\beta} - \boldsymbol{\beta}_h\|_{1,K} + \|\boldsymbol{\beta} - \boldsymbol{\beta}_h\|_{0,K}.
\end{aligned} \tag{4.19}$$

The assertion now follows from the estimates (4.17)–(4.19). □

Let us close this section by briefly discussing this result. From above we get the global estimate

$$\begin{aligned}
\|\nabla(I_h w - w_h)\|_0 \le C\big(&\|\boldsymbol{\beta} - \boldsymbol{\beta}_h\|_0 + t^2\|\boldsymbol{q} - \boldsymbol{R}_h\boldsymbol{q}\|_0 \\
&+ (h + t)(\|\boldsymbol{\beta} - \boldsymbol{\beta}_h\|_1 + t\|\boldsymbol{q} - \boldsymbol{q}_h\|_0)\big).
\end{aligned} \tag{4.20}$$

For the case of convex domain and clamped boundary conditions Theorem 3.2 gives the convergence rates

$$\|w - w_h\|_1 + \|\boldsymbol{\beta} - \boldsymbol{\beta}_h\|_1 + t\|\boldsymbol{q} - \boldsymbol{q}_h\|_0 = \mathcal{O}(h_i^k + h_b) \tag{4.21}$$

and

$$\|\boldsymbol{\beta} - \boldsymbol{\beta}_h\|_0 = \mathcal{O}\big(h(h_i^k + h_b)\big). \tag{4.22}$$

Lemma 4.4 gives

$$t\|\boldsymbol{q} - \boldsymbol{R}_h\boldsymbol{q}\|_0 = \mathcal{O}\big(h_i^k + h_b\big). \tag{4.23}$$

Hence, we obtain

$$\|w_h - I_h w\|_1 = \mathcal{O}\big((h + t)(h_i^k + h_b)\big). \tag{4.24}$$

and we see that the convergence rate for $\|w_h - I_h w\|_1$ is by the factor $h + t$ better than the rate for both $\|w - w_h\|_1$ (see Theorem 3.2) and $\|w - I_h w\|_1$ (Lemma 4.2). Since $I_h w$ interpolates w at the vertices (cf. (4.1)) this also gives an indication that the vertex values of w_h are converging with an improved speed. The numerical results in Section 6 verify this. Let us also remark that in practice we are interested in the case when $t < h$ since for a finer mesh the error in the model (with respect to the three dimensional structure) is greater than the discretization error.

5 The postprocessing method

In the postprocessing we construct an improved approximation for the deflection in the space

$$W_h^* = \{v \in W \mid v_{|K} \in P_{k+1}(K) \ \ \forall K \in \mathcal{C}_h\}. \tag{5.1}$$

To define the postprocessing we first introduce the corresponding interpolation operator $I_h^* : H^s(\Omega) \to W_h^*$, $s > 1$:

$$\begin{aligned} &(v - I_K^* v)(a) = 0 \ \text{ for every vertex } a \in K, \\ &\langle v - I_K^* v, p\rangle_E = 0 \ \ \forall p \in P_{k-1}(E) \ \ \forall E \subset K, \\ &(v - I_K^* v, p)_K = 0 \ \ \forall p \in P_{k-2}(K), \end{aligned} \tag{5.2}$$

for $I_K^* = I_{h|K}^* \ \ \forall K \in \mathcal{C}_h$.

Lemma 5.1. *There is a positive constant C such that*

$$\|w - I_h^* w\|_1 \le C(h+t)\{h_i^k(\|g\|_{k-2} + t\|g\|_{k-1}) + h_b(\|g\|_{-1} + t\|g\|_0)\}. \tag{5.3}$$

Proof. In contrast to the proof of Lemma 4.2 we now have to split $w = w_0 + w_r$. We write

$$\begin{aligned} \|w - I_h^* w\|_1 &= \|w_0 - I_h^* w_0 + w_r - I_h^* w_r\|_1 \\ &\le \|w_0 - I_h^* w_0\|_1 + \|w_r - I_h^* w_r\|_1. \end{aligned} \tag{5.4}$$

For the first term we get, using Lemma 4.1 with k replaced with $k+1$ and Theorem 3.1,

$$\begin{aligned} \|w_0 - I_h^* w_0\|_1 &\le \|w_0 - I_h^* w_0\|_{1,\Omega_i} + \|w_0 - I_h^* w_0\|_{1,\Omega_b} \\ &\le C\big(h_i^{k+1}\|w_0\|_{k+2,\Omega_i} + h_b^2\|w_0\|_{3,\Omega_b}\big) \\ &\le Ch\big(h_i^k\|w_0\|_{k+2,\Omega_i} + h_b\|w_0\|_{3,\Omega_b}\big) \\ &\le Ch\big(h_i^k(\|g\|_{k-2} + t\|g\|_{k-1}) + h_b(\|g\|_{-1} + t\|g\|_0)\big). \end{aligned} \tag{5.5}$$

For the second term we get

$$\begin{aligned} \|w_r - I_h^* w_r\|_1 &\le \|w_r - I_h^* w_r\|_{1,\Omega_i} + \|w_r - I_h^* w_r\|_{1,\Omega_b} \\ &\le C\big(h_i^k\|w_r\|_{k+1,\Omega_i} + h_b\|w_r\|_{2,\Omega_b}\big) \\ &\le Ct\big(h_i^k(\|g\|_{k-2} + t\|g\|_{k-1}) + h_b(\|g\|_{-1} + t\|g\|_0)\big). \end{aligned} \tag{5.6}$$

Combining the above two estimates gives the assertion. □

Next, we note that the interpolation operators I_h^* and I_h are hierarchical, i.e. I_K^* is obtained from I_K by adding the degrees of freedom

$$\langle v - I_K^* v, p\rangle_E = 0 \ \ \forall p \in \tilde{P}_{k-1}(E) \ \ \forall E \subset K, \tag{5.7}$$

$$(v - I_K^* v, p)_K = 0 \ \ \forall p \in \tilde{P}_{k-2}(K), \tag{5.8}$$

where as before the tilde denotes homogeneous polynomials. This motivates the following notation

$$\widehat{W}(K) = \{v \in P_{k+1}(K) \mid I_K v = 0,\ (v,p)_K = 0\ \ \forall p \in \tilde{P}_{k-2}(K)\} \tag{5.9}$$

$$\begin{aligned}\overline{W}(K) = \{v \in P_{k+1}(K) \mid I_K v = 0,\ \langle v,p\rangle_E = 0 \\ \forall p \in \tilde{P}_{k-1}(E)\ \ \forall E \subset K\}\end{aligned} \tag{5.10}$$

and the splitting

$$P_{k+1}(K) = P_k(K) \oplus \widehat{W}(K) \oplus \overline{W}(K). \tag{5.11}$$

We then define the

Postprocessing scheme 5.1. *For all triangles $K \in \mathcal{C}_h$ find the local postprocessed finite element deflection $w^*_{h|K} \in P_{k+1}(K) = P_k(K) \oplus \widehat{W}(K) \oplus \overline{W}(K)$ such that*

$$I_h w^*_{h|K} = w_{h|K}, \tag{5.12}$$

$$\begin{aligned}\langle \nabla w^*_h \cdot \boldsymbol{\tau}_E, \nabla \hat{v} \cdot \boldsymbol{\tau}_E\rangle_E &= \langle (\boldsymbol{\beta}_h + t^2 \boldsymbol{q}_h) \cdot \boldsymbol{\tau}_E, \nabla \hat{v} \cdot \boldsymbol{\tau}_E\rangle_E \\ &\forall E \subset \partial K, \quad \forall \hat{v} \in \widehat{W}(K),\end{aligned} \tag{5.13}$$

$$(\nabla w^*_h, \nabla \bar{v})_K = (\boldsymbol{\beta}_h + t^2 \boldsymbol{q}_h, \nabla \bar{v})_K\ \ \forall \bar{v} \in \overline{W}(K). \tag{5.14}$$

Here it should be pointed out that the postprocessed deflection is conforming since $(\boldsymbol{\beta}_h + t^2 \boldsymbol{q}_h) \cdot \boldsymbol{\tau}$ is continuous along inter element boundaries.

Remark 5.1. If we write $w^*_h = w_h + w^d_h$, the improvement w^d_h is computed from the equations

$$\begin{aligned}\langle \nabla w^d_h \cdot \boldsymbol{\tau}_E, \nabla \hat{v} \cdot \boldsymbol{\tau}_E\rangle_E &= \langle (\boldsymbol{\beta}_h + t^2 \boldsymbol{q}_h - \nabla w_h) \cdot \boldsymbol{\tau}_E, \nabla \hat{v} \cdot \boldsymbol{\tau}_E\rangle_E \\ &\forall E \subset \partial K, \quad \forall \hat{v} \in \widehat{W}(K), \\ (\nabla w^d_h, \nabla \bar{v})_K &= (\boldsymbol{\beta}_h + t^2 \boldsymbol{q}_h - \nabla w_h, \nabla \bar{v})_K\ \ \forall \bar{v} \in \overline{W}(K).\end{aligned} \tag{5.15}$$

It holds

Lemma 5.2. *The system* (5.15) *has a unique solution.*

Proof. By linearity we have to show that if $\langle \nabla z_h \cdot \boldsymbol{\tau}_E, \nabla \hat{v} \cdot \boldsymbol{\tau}_E\rangle_E = 0$ and $(\nabla z_h, \nabla \bar{v})_K = 0$, then $z_h = 0$. To this end we first choose $\hat{v} \in \widehat{W}(K)$ such that $\hat{v}_{|\partial K} = z_{h|\partial K}$ and the first relation implies that $z_{h|\partial K} = 0$. Hence, $z_h \in \overline{W}(K)$ and we can choose $\bar{v} = z_h$ in the second condition which then implies the assertion. □

To derive the error estimate for the postprocessing we need the following stability result.

Lemma 5.3. *For every $v \in \widehat{W}(K) \oplus \overline{W}(K)$ there exist $\hat{v} \in \widehat{W}(K)$ and $\bar{v} \in \overline{W}(K)$, with*

$$\big(h_K^{1/2} \sum_{E \subset \partial K} \|\nabla \hat{v} \cdot \boldsymbol{\tau}_E\|_{0,E} + \|\nabla \bar{v}\|_{0,K}\big) \le C,$$

such that

$$\|\nabla v\|_{0,K} \leq h_K \sum_{E\subset\partial K} \langle \nabla v\cdot\boldsymbol{\tau}_E, \nabla\hat{v}\cdot\boldsymbol{\tau}_E\rangle_E + (\nabla v, \nabla\bar{v})_K.$$

Proof. By Lemma 5.2

$$\sup_{\hat{v}\in\widehat{W}(K),\ \bar{v}\in\overline{W}(K)} \frac{h_K\sum_{E\subset\partial K}\langle \nabla v\cdot\boldsymbol{\tau}_E, \nabla\hat{v}\cdot\boldsymbol{\tau}_E\rangle_E + (\nabla v,\nabla\bar{v})_K}{h_K^{1/2}\sum_{E\subset\partial K}\|\nabla\hat{v}\cdot\boldsymbol{\tau}_E\|_{0,E} + \|\nabla\bar{v}\|_{0,K}} \tag{5.16}$$

defines a norm in $\widehat{W}(K)\oplus\overline{W}(K)$. By local scaling this is equivalent to $\|\nabla v\|_{0,K}$ and the assertion is simply a reformulation of this. □

We will also need the following result which is easily proved by scaling.

Lemma 5.4. *Let E be an edge of K. Then there exists a constant $C>0$ such that*

$$h_K^{1/2}\|\boldsymbol{p}\cdot\boldsymbol{\tau}_E\|_{0,E} \leq C\|\boldsymbol{p}\|_{0,K}\ \ \forall\boldsymbol{p}\in[P_k(K)]^2\oplus[B_{k+1}(K)]^2, \tag{5.17}$$

where $k\geq 0$.

Further, let us define the reduction operator $\boldsymbol{R}_h^*$ for the index $k+1$ to the space

$$\boldsymbol{Q}_h^* = \{\,\boldsymbol{r}\in\boldsymbol{H}(\mathrm{rot}:\Omega)\mid \boldsymbol{r}_{|K}\in[P_k(K)]^2\oplus(y,-x)\tilde{P}_k(K)\ \forall K\in\mathcal{C}_h\,\}. \tag{5.18}$$

It is defined through the conditions

$$\langle(\boldsymbol{R}_K^*\boldsymbol{\eta}-\boldsymbol{\eta})\cdot\boldsymbol{\tau}_E, p\rangle_E = 0\ \ \forall p\in P_k(E)\ \ \forall E\subset\partial K, \tag{5.19}$$

$$(\boldsymbol{R}_K^*\boldsymbol{\eta}-\boldsymbol{\eta},\boldsymbol{p})_K = 0\ \ \forall\boldsymbol{p}\in[P_{k-1}(K)]^2, \tag{5.20}$$

which have to be satisfied by the local operator $\boldsymbol{R}_K^* = \boldsymbol{R}_{h|K}^*\ \ \forall K\in\mathcal{C}_h$.

We are now ready to prove the error estimate for the postprocessing. Here we will use the relationship

$$\boldsymbol{R}_h^*\nabla v = \nabla I_h^* v\ \ \forall v\in H^s(\Omega),\ s\geq 2. \tag{5.21}$$

Lemma 5.5. *There is a positive constant C such that*

$$\begin{aligned}\|\nabla(w-w_h^*)\|_{0,K} \leq C\{&\|\nabla(I_h w-w_h)\|_{0,K} + \|\nabla(w-I_h^*w)\|_{0,K}\\ &+\|\boldsymbol{\beta}-\boldsymbol{\beta}_h\|_{0,K} + t^2\|\boldsymbol{q}-\boldsymbol{q}_h\|_{0,K}\\ &+\|\boldsymbol{\beta}-\boldsymbol{R}_h^*\boldsymbol{\beta}\|_{0,K} + t^2\|\boldsymbol{q}-\boldsymbol{R}_h^*\boldsymbol{q}\|_{0,K}\}.\end{aligned} \tag{5.22}$$

Proof. We write $I_h^*w = I_hw + I_h^d w$ and by the triangle inequality we get

$$\begin{aligned}\|\nabla(I_h^*w-w_h^*)\|_{0,K} &= \|\nabla(I_hw-w_h+I_h^dw-w_h^d)\|_{0,K}\\ &\leq \|\nabla(I_hw-w_h)\|_{0,K} + \|\nabla(I_h^dw-w_h^d)\|_{0,K}.\end{aligned} \tag{5.23}$$

Since $I_h^d w - w_h^d \in \widehat{W}(K) \oplus \overline{W}(K)$ Lemma 5.3 implies that there exist $\hat{v} \in \widehat{W}(K)$ and $\bar{v} \in \overline{W}(K)$, with

$$\big(h_K^{1/2} \sum_{E\subset\partial K} \|\nabla\hat{v}\cdot\boldsymbol{\tau}_E\|_{0,E} + \|\nabla\bar{v}\|_{0,K}\big) \le C, \tag{5.24}$$

such that

$$\|\nabla(I_h^d w - w_h^d)\|_{0,K} \le h_K \sum_{E\subset\partial K} \langle\nabla(I_h^d w - w_h^d)\cdot\boldsymbol{\tau}_E, \nabla\hat{v}\cdot\boldsymbol{\tau}_E\rangle_E + (\nabla(I_h^d w - w_h^d), \nabla\bar{v})_K. \tag{5.25}$$

Next, we write

$$\begin{aligned} h_K &\sum_{E\subset\partial K} \langle\nabla(I_h^d w - w_h^d)\cdot\boldsymbol{\tau}_E, \nabla\hat{v}\cdot\boldsymbol{\tau}_E\rangle_E + (\nabla(I_h^d w - w_h^d), \nabla\bar{v})_K \qquad (5.26)\\ &= h_K \sum_{E\subset\partial K} \langle\nabla(I_h^* w - w_h^*)\cdot\boldsymbol{\tau}_E, \nabla\hat{v}\cdot\boldsymbol{\tau}_E\rangle_E + (\nabla(I_h^* w - w_h^*), \nabla\bar{v})_K \\ &\quad -h_K \sum_{E\subset\partial K} \langle\nabla(I_h w - w_h)\cdot\boldsymbol{\tau}_E, \nabla\hat{v}\cdot\boldsymbol{\tau}_E\rangle_E - (\nabla(I_h w - w_h), \nabla\bar{v})_K. \end{aligned}$$

Using (5.24) and Lemma 5.4 the second term is readily estimated

$$\begin{aligned} \Big| h_K &\sum_{E\subset\partial K} \langle\nabla(I_h w - w_h)\cdot\boldsymbol{\tau}_E, \nabla\hat{v}\cdot\boldsymbol{\tau}_E\rangle_E + (\nabla(I_h w - w_h), \nabla\bar{v})_K \Big| \\ &\le C\|\nabla(I_h w - w_h)\|_{0,K}. \end{aligned} \tag{5.27}$$

Next, using (5.21), (2.7), (5.13), (5.14), (5.24) and Lemma 5.4 we have

$$\begin{aligned} h_K &\sum_{E\subset\partial K} \langle\nabla(I_h^* w - w_h^*)\cdot\boldsymbol{\tau}_E, \nabla\hat{v}\cdot\boldsymbol{\tau}_E\rangle_E + (\nabla(I_h^* w - w_h^*), \nabla\bar{v})_K \\ &= h_K \sum_{E\subset\partial K} \langle(\boldsymbol{R}_h^*(\boldsymbol{\beta} + t^2\boldsymbol{q}) - (\boldsymbol{\beta}_h + t^2\boldsymbol{q}_h))\cdot\boldsymbol{\tau}_E, \nabla\hat{v}\cdot\boldsymbol{\tau}_E\rangle_E \\ &\qquad +(\boldsymbol{R}_h^*(\boldsymbol{\beta} + t^2\boldsymbol{q}) - (\boldsymbol{\beta}_h + t^2\boldsymbol{q}_h), \nabla\bar{v})_K \qquad (5.28)\\ &= h_K \sum_{E\subset\partial K} \langle(\boldsymbol{R}_h^*\boldsymbol{\beta} - \boldsymbol{\beta}_h + t^2(\boldsymbol{R}_h^*\boldsymbol{q} - \boldsymbol{q}_h))\cdot\boldsymbol{\tau}_E, \nabla\hat{v}\cdot\boldsymbol{\tau}_E\rangle_E \\ &\qquad +(\boldsymbol{R}_h^*\boldsymbol{\beta} - \boldsymbol{\beta}_h + t^2(\boldsymbol{R}_h^*\boldsymbol{q} - \boldsymbol{q}_h), \nabla\bar{v})_K \\ &\le h_K \sum_{E\subset\partial K} \|(\boldsymbol{R}_h^*\boldsymbol{\beta} - \boldsymbol{\beta}_h + t^2(\boldsymbol{R}_h^*\boldsymbol{q} - \boldsymbol{q}_h))\cdot\boldsymbol{\tau}_E\|_{0,E}\|\nabla\hat{v}\cdot\boldsymbol{\tau}_E\|_{0,E} \\ &\qquad +\|\boldsymbol{R}_h^*\boldsymbol{\beta} - \boldsymbol{\beta}_h + t^2(\boldsymbol{R}_h^*\boldsymbol{q} - \boldsymbol{q}_h)\|_{0,K}\|\nabla\bar{v}\|_{0,K} \\ &\le Ch_K^{1/2} \sum_{E\subset\partial K} \|(\boldsymbol{R}_h^*\boldsymbol{\beta} - \boldsymbol{\beta}_h + t^2(\boldsymbol{R}_h^*\boldsymbol{q} - \boldsymbol{q}_h))\cdot\boldsymbol{\tau}_E\|_{0,E} \\ &\qquad +\|\boldsymbol{R}_h^*\boldsymbol{\beta} - \boldsymbol{\beta}_h + t^2(\boldsymbol{R}_h^*\boldsymbol{q} - \boldsymbol{q}_h)\|_{0,K} \\ &\le C\|\boldsymbol{R}_h^*\boldsymbol{\beta} - \boldsymbol{\beta}_h + t^2(\boldsymbol{R}_h^*\boldsymbol{q} - \boldsymbol{q}_h)\|_{0,K}. \end{aligned}$$

Finally, we use the triangle inequality to obtain

$$\begin{aligned} \|\boldsymbol{R}_h^*\boldsymbol{\beta} &- \boldsymbol{\beta}_h + t^2(\boldsymbol{R}_h^*\boldsymbol{q} - \boldsymbol{q}_h)\|_{0,K} \qquad (5.29)\\ &\le \|\boldsymbol{\beta} - \boldsymbol{\beta}_h\|_{0,K} + \|\boldsymbol{\beta} - \boldsymbol{R}_h^*\boldsymbol{\beta}\|_{0,K} \\ &\quad +t^2\|\boldsymbol{q} - \boldsymbol{R}_h^*\boldsymbol{q}\|_{0,K} + t^2\|\boldsymbol{q} - \boldsymbol{q}_h\|_{0,K}. \end{aligned}$$

The assertion now follows by collecting the above estimates and using the triangle inequality. □

By combining Lemma 5.5 and Theorem 4.1 we get the following estimate.

Theorem 5.1. *There is a positive constant C such that*

$$\begin{aligned}\|\nabla(w-w_h^*)\|_{0,K}&\\ \le C\{&h_K\|\boldsymbol{\beta}-\boldsymbol{\beta}_h\|_{1,K}+\|\boldsymbol{\beta}-\boldsymbol{\beta}_h\|_{0,K}+t^2\|\boldsymbol{q}-\boldsymbol{q}_h\|_{0,K}\\ &+\|\nabla(w-I_h^*w)\|_{0,K}+\|\boldsymbol{\beta}-\boldsymbol{R}_h^*\boldsymbol{\beta}\|_{0,K}\\ &+t^2\|\boldsymbol{q}-\boldsymbol{R}_h^*\boldsymbol{q}\|_{0,K}+t^2\|\boldsymbol{q}-\boldsymbol{R}_h\boldsymbol{q}\|_{0,K}\}.\end{aligned}\tag{5.30}$$

□

We point out that this results is local for one element. It is made up of two parts. The first term $h_K\|\boldsymbol{\beta}-\boldsymbol{\beta}_h\|_{1,K}+\|\boldsymbol{\beta}-\boldsymbol{\beta}_h\|_{0,K}+t^2\|\boldsymbol{q}-\boldsymbol{q}_h\|_{0,K}$ is related to the error of the original method. We note that the natural norm of the local error is $\|\boldsymbol{\beta}-\boldsymbol{\beta}_h\|_{1,K}+t\|\boldsymbol{q}-\boldsymbol{q}_h\|_{0,K}$. Hence we for this get an improvement with the factor h_K+t. Also, the term $\|\boldsymbol{\beta}-\boldsymbol{\beta}_h\|_{0,K}$ is in general smaller than $\|\boldsymbol{\beta}-\boldsymbol{\beta}_h\|_{1,K}$.

The second term consists of interpolation estimates which all are a factor h_K+t better that the interpolation estimates needed for the a-priori analysis, see the proof below.

For the case of a clamped plate and a convex domain we get the result:

Theorem 5.2. *Let Ω be a convex polygon and suppose that the plate is clamped. For $g\in H^{k-2}(\Omega)$, $tg\in H^{k-1}(\Omega)$ it then holds*

$$\|w-w_h^*\|_1\le C(h+t)\{h_i^k(\|g\|_{k-2}+t\|g\|_{k-1})+h_b(\|g\|_{-1}+t\|g\|_0)\}\tag{5.31}$$

Proof. From the preceding theorem we have

$$\begin{aligned}\|\nabla(w-w_h^*)\|_1\le C\big(&h\|\boldsymbol{\beta}-\boldsymbol{\beta}_h\|_1+\|\boldsymbol{\beta}-\boldsymbol{\beta}_h\|_0+t^2\|\boldsymbol{q}-\boldsymbol{q}_h\|_0\big)\\ &+C\big(\|\nabla(w-I_h^*w)\|_0+\|\boldsymbol{\beta}-\boldsymbol{R}_h^*\boldsymbol{\beta}\|_0\\ &+t^2\|\boldsymbol{q}-\boldsymbol{R}_h^*\boldsymbol{q}\|_0+t^2\|\boldsymbol{q}-\boldsymbol{R}_h\boldsymbol{q}\|_0\big).\end{aligned}\tag{5.32}$$

The first four terms are estimated by Theorem 3.2 and Lemma 5.1 giving the improvement by the factor $h+t$. For the next two terms we use Lemma 4.3 with k replaced with $k+1$. We obtain

$$\|\boldsymbol{\beta}-\boldsymbol{R}_h^*\boldsymbol{\beta}\|_{0,K}\le Ch_K^{k+1}\|\boldsymbol{\beta}\|_{k+1,K},\quad t^2\|\boldsymbol{q}-\boldsymbol{R}_h^*\boldsymbol{q}\|_{0,K}\le t^2Ch_K^k\|\boldsymbol{q}\|_{k,K},\tag{5.33}$$

for $K\subset\Omega_i$, and

$$\|\boldsymbol{\beta}-\boldsymbol{R}_h^*\boldsymbol{\beta}\|_{0,K}\le Ch_K^2\|\boldsymbol{\beta}\|_{2,K},\quad t^2\|\boldsymbol{q}-\boldsymbol{R}_h^*\boldsymbol{q}\|_{0,K}\le t^2Ch_K\|\boldsymbol{q}\|_{1,K},\tag{5.34}$$

for $K\subset\Omega_b$. For the last term we also use Lemma 4.3. The assertion follows from the regularity estimates of Theorem 3.1. □

6 Numerical Results

Our numerical computations are performed for a test problem for which an analytical solution has been obtained by Arnold and Falk [1]. The domain is the semi-infinite region $\Omega = \{(x, y) \in \mathbb{R}^2 \mid y > 0\}$ and the loading is $g = \frac{1}{G}\cos x$. The solution of the problem is

$$\begin{aligned} w &= \{1/A + \lambda^{-1}t^2 + ae^{-y} + b(2A\lambda^{-1}t^2 + y)e^{-y} - c\lambda^{-1}t^2e^{-y}\}\cos x, \\ \beta_x &= \{-1/A - ae^{-y} - bye^{-y} + c\lambda^{-1}t^2e^{-y} - d\gamma\lambda^{-1}te^{-\gamma y/t}\}\sin x, \\ \beta_y &= \{-ae^{-y} + b(1-y)e^{-y} + c\lambda^{-1}t^2e^{-y} - d\lambda^{-1}t^2e^{-\gamma y/t}\}\cos x, \end{aligned} \tag{6.1}$$

where $A = G/(6(1-\nu))$, $\gamma = \sqrt{12\kappa + t^2}$ with the shear corrector factor κ. The coefficients a, b, c, d (which depend on G, ν and t) are given in reference [1] for five different types of boundary conditions on $\Gamma = \{(x, y) \in \mathbb{R}^2 \mid y = 0\}$.

In our computations we have chosen $\nu = 0.3$, $G = 1/(2(1+\nu))$, $\kappa = 1$, $t = 0.01$, and we consider three different boundary conditions: hard clamped, hard simply supported and free.

In references [2] and [3] the boundary layer behavior is studied by using asymptotic expansions in powers of the plate thickness. The edge effects are shown to be of different order for different boundary conditions; the weakest layer appears in the soft clamped case whereas the free and soft simply supported cases have the strongest layers.

In the computations we use the domain $D = (0, \pi/2) \times (0, 3\pi/2)$. Along the boundaries $x = 0$, $x = \pi/2$ and $y = 3\pi/2$, we impose the Dirichlet boundary conditions obtained from the exact solution (6.1).

Most of the results are calculated by using uniform meshes, but in the end of the paper we also give some results for general, non-uniform, meshes.

The number of elements in the x-direction of the discretized domain is $N = 2, 4, 6$ or 8, see Figures 1 and 2. The mesh size is $h \approx 1/N$ and the degree of the elements used is $k = 2$ (quadratic) or $k = 3$ (cubic).

In order to study the accuracy in the interior of the domain and near the boundary we give the relative errors, measured in the H^1-norm and in the L^2-norm, in the subdomains $D_i = \{(x, y) \in D \mid y \in (\pi, 5\pi/4)\}$ and $D_b = \{(x, y) \in D \mid y \in (0, \pi/4)\}$; yellow and magenta, respectively, in Figure 1.

The results for the interior region are shown in Figures 3–5, and the results for the boundary region in Figures 6–11, respectively. The relative errors of the original finite element deflection (the dashed red lines) and the postprocessed finite element deflection (the solid black lines) are on the logarithmic scale with respect to N.

To study the convergence rate function of the form $CN^{-r} \approx Ch^r$ is fitted to the results using least squares. The fitted lines with the slopes r and r^*, for the original and for the postprocessed deflections, are also shown in the figures, and listed in Table 1.

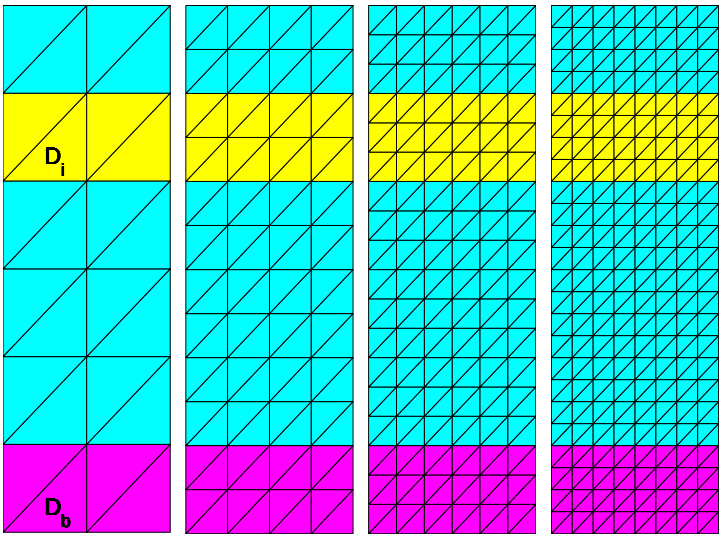

Figure 1: The uniform meshes with $N = 2, 4, 6, 8$; Interior region D_i; Boundary region D_b.

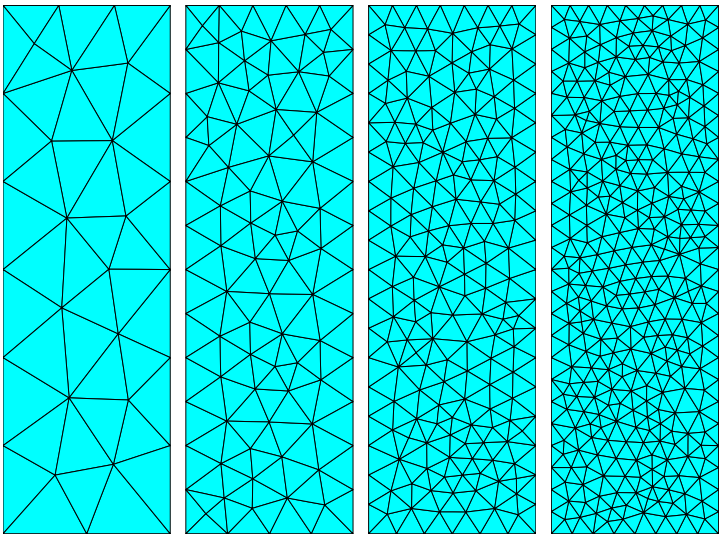

Figure 2: The non-uniform meshes with $N = 2, 4, 6, 8$.

6.1 The accuracy in the interior region

In the interior region for the clamped boundary the numerical results in Figure 3 are clearly in accordance with the theory: In the H^1-norm the convergence rate of the original finite element deflection is $r \approx k$ and the convergence rate of the postprocessed finite element deflection is $r^* \approx k + 1 \approx r + 1$ – there is a slope change when comparing the solid line and the corresponding dashed line. This means that the desired one additional power of the mesh size h (or $h+t$) is reached. For the simply supported and the free boundaries the situation is almost identical, see Figures 4 and 5 and Table 1.

The behavior in the L^2-norm is almost similar: For the clamped edge $r \approx k + 1$ and $r^* \approx k + 2 \approx r + 1$. For the simply supported and the free edge the convergence rates of the postprocessed deflection are closer to $r^* \approx k + 3/2 \approx r + 1/2$.

We remark that to rigorously prove an increased accuracy in the L^2-norm seems to be difficult due to the t-dependency of the solution and the boundary layers.

Table 1: Interior region; Uniform mesh; Convergence rates in Figures 3, 4 and 5 (h^r for the original , h^{r^*} for the postprocessed deflection; C for clamped, SS for simly supported, F for free edge).

Boundary condition	C	C	SS	SS	F	F
Norm	H^1	L^2	H^1	L^2	H^1	L^2
$k = 2$						
r	2.0	3.1	2.0	3.0	2.0	3.0
r^*	3.1	4.1	3.1	4.1	3.0	4.0
$k = 3$						
r	3.0	4.0	3.0	4.0	3.0	4.0
r^*	4.1	4.8	4.1	4.7	4.1	4.6

6.2 The accuracy in the boundary region

In the boundary region the numerical results in Figures 6, 7, and 8 reflect the strength of the edge effect: For the clamped and simply supported edges the convergence – especially in the H^1-norm – is almost as good as in the interior region, and the effect of the boundary layer is only slightly seen, see Figures 6 and 7.

For the free edge the rate of convergence rapidly slows down for both the original and the postprocessed deflection, which is clearly seen in Figure 8. The convergence rate seems to be of order $\mathcal{O}(h^{1/2})$ – for both the original and the postprocessed deflection. In [12, 7] the rate for the original deflection in the H^1-norm is shown to be of that order and now it seems that the same rate is valid also for the L^2-norm. Furthermore, the same rate appears to be

valid also for the original finite element rotation in the L^2-norm, see Figure 9. Actually, this seem to be the reason why also the convergence rate for the postprocessed deflection is the same; the L^2-norm of the finite element rotation appears in the error estimates for the postprocessed deflection, see Theorem 5.1.

Although the convergence of the relative errors in the H^1-norm and the L^2-norm slows down near the free boundary, we see that an improvement is obtained for coarse meshes. (For quadratic elements this is significant.) This is also seen in Figures 10 and 11 in which the distributions of the pointwise errors of the original (dashed red line) and the postprocessed finite element deflections (solid black line) are plotted.

For quadratic elements with the mesh size $N = 4$ the pointwise errors are plotted in the y-direction along the line $x = \pi/4$ and in the x-direction along the line $y = \pi/4$ in Figure 10. For cubic elements with the mesh size $N = 2$ the corresponding errors are plotted in Figure 11. In the figures the superconvergence of the vertex values (marked with triangles) is clearly seen in the both cases.

6.3 The accuracy for non-uniform meshes

The non-uniform meshes we have used are shown in Figure 2. For these meshes our results are for the clamped case with quadratic elements ($k = 2$). Here the relative errors, measured in the H^1-norm and in the L^2-norm, are calculated in the whole discretized domain. There was no significant difference between the interior and the boundary region in the corresponding case for the uniform meshes, but in principle, the results should follow the behavior in the boundary region that is the dominating region for the errors.

The numerical results in Figure 12 are very similar to those for the uniform meshes in the boundary region, see Figure 6. So, in the errors for the original and the postprocessed deflection there is no essential dependence on the mesh distortion of reasonable order.

References

[1] D. N. Arnold and R. S. Falk. Edge effects in the Reissner–Mindlin plate theory. In A. K. Noor, T. Belytschko, and J. C. Simo, editors, *Analytic and Computational Models of Shells.*, pages 71–90, New York, 1989. ASME.

[2] D. N. Arnold and R. S. Falk. The boundary layer for the Reissner–Mindlin plate model. *SIAM J. Math. Anal.*, 21:281–312, 1990.

[3] D. N. Arnold and R. S. Falk. Asymptotic analysis of the boundary layer for the Reissner–Mindlin plate model. *SIAM J. Math. Anal.*, 27:486–514, 1996.

[4] K.-J. Bathe, F. Brezzi, and M. Fortin. Mixed-interpolated elements for Reissner–Mindlin plates. *Int. J. Num. Meths. Eng.*, 28:1787–1801, 1989.

[5] F. Brezzi and M. Fortin. *Mixed and Hybrid Finite Element Methods.* Springer Verlag, New York, 1991.

[6] F. Brezzi, M. Fortin, and R. Stenberg. Error analysis of mixed-interpolated elements for Reissner–Mindlin plates. *Mathematical Models and Methods in Applied Sciences*, 1:125–151, 1991.

[7] L. Beirao da Veiga. Finite element methods for a modified Reissner–Mindlin free plate model. *SIAM J. Num. Anal.*, 42:1572–1591, 2004.

[8] V. Girault and P.-A. Raviart. *Finite Element Methods for Navier-Stokes Equations. Theory and Algorithms.* Springer-Verlag, 1986.

[9] M. Lyly, J. Niiranen, and R. Stenberg. A refined error analysis of the MITC plate elements. *In preparation.*

[10] P. Peisker and D. Braess. Uniform convergence of mixed interpolated elements for Reissner–Mindlin plates. M^2AN, 26:557–574, 1992.

[11] J. Pitkäranta. Analysis of some low-order finite element schemes for Mindlin–Reissner and Kirchhoff plates. *Numer. Math.*, 53:237–254, 1988.

[12] J. Pitkäranta and M. Suri. Design principles and error analysis for reduced-shear plate-bending finite elements. *Numer. Math.*, 75:223–266, 1996.

[13] P.-A. Raviart and J. M. Thomas. A mixed finite element method for second order elliptic problems. In *Mathematical Aspects of the Finite Element Method. Lecture Notes in Math. 606*, pages 292–315. Springer-Verlag, 1977.

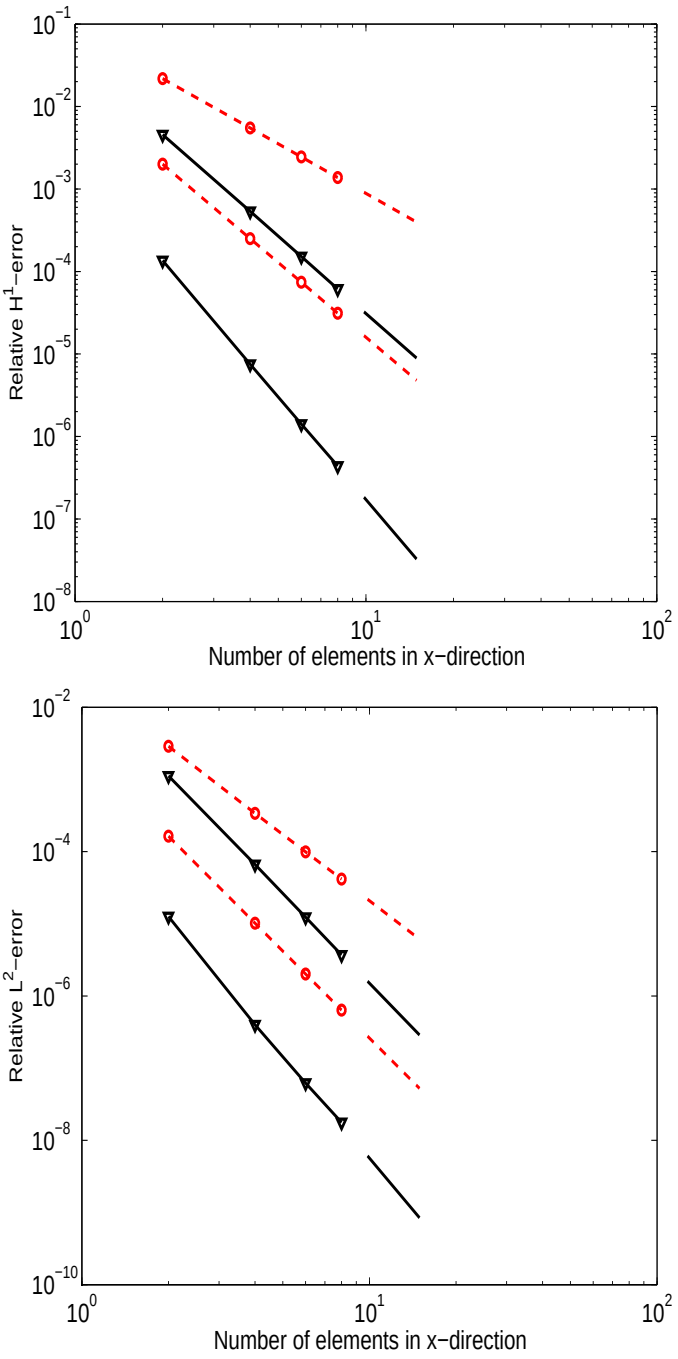

Figure 3: Clamped edge; Interior region; Uniform mesh; Convergence of the relative H^1- and L^2-errors with $k = 2, 3$ (red dashed line for the original, black solid line for the postprocessed deflection).

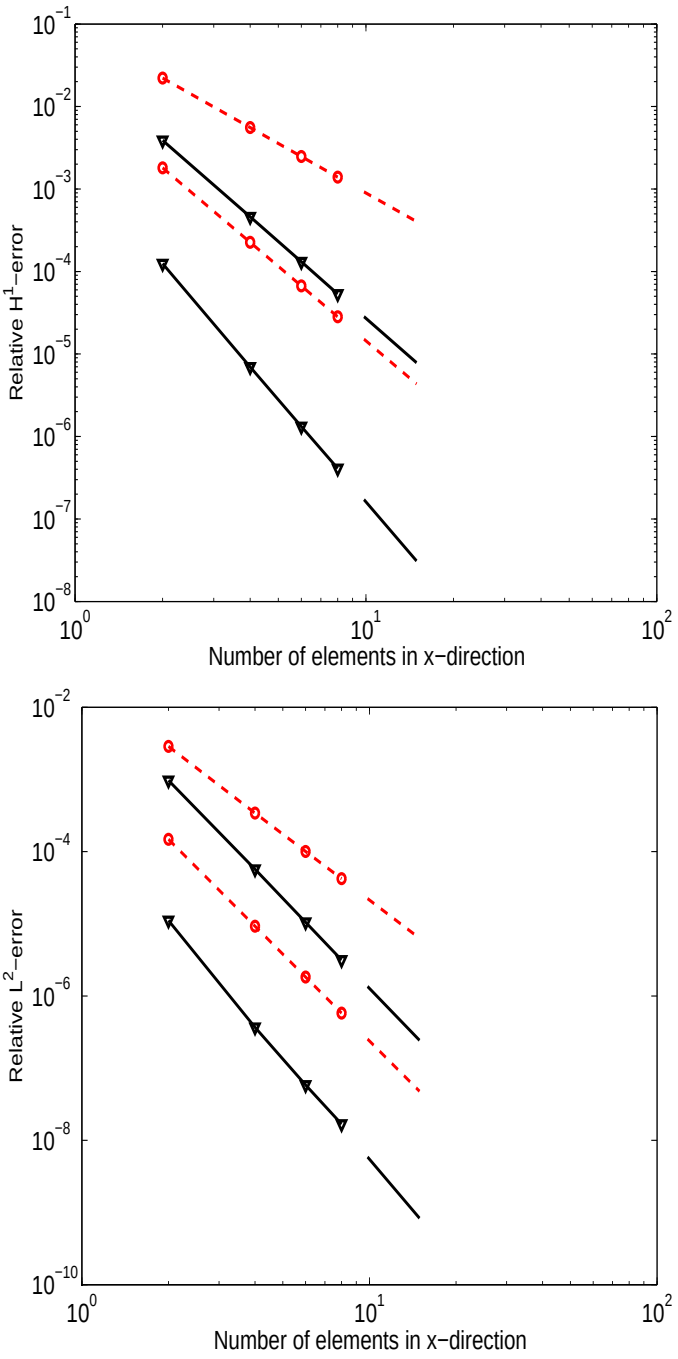

Figure 4: Simply supported edge; Interior region; Uniform mesh; Convergence of the relative H^1- and L^2-errors with $k = 2, 3$ (red dashed line for the original, black solid line for the postprocessed deflection).

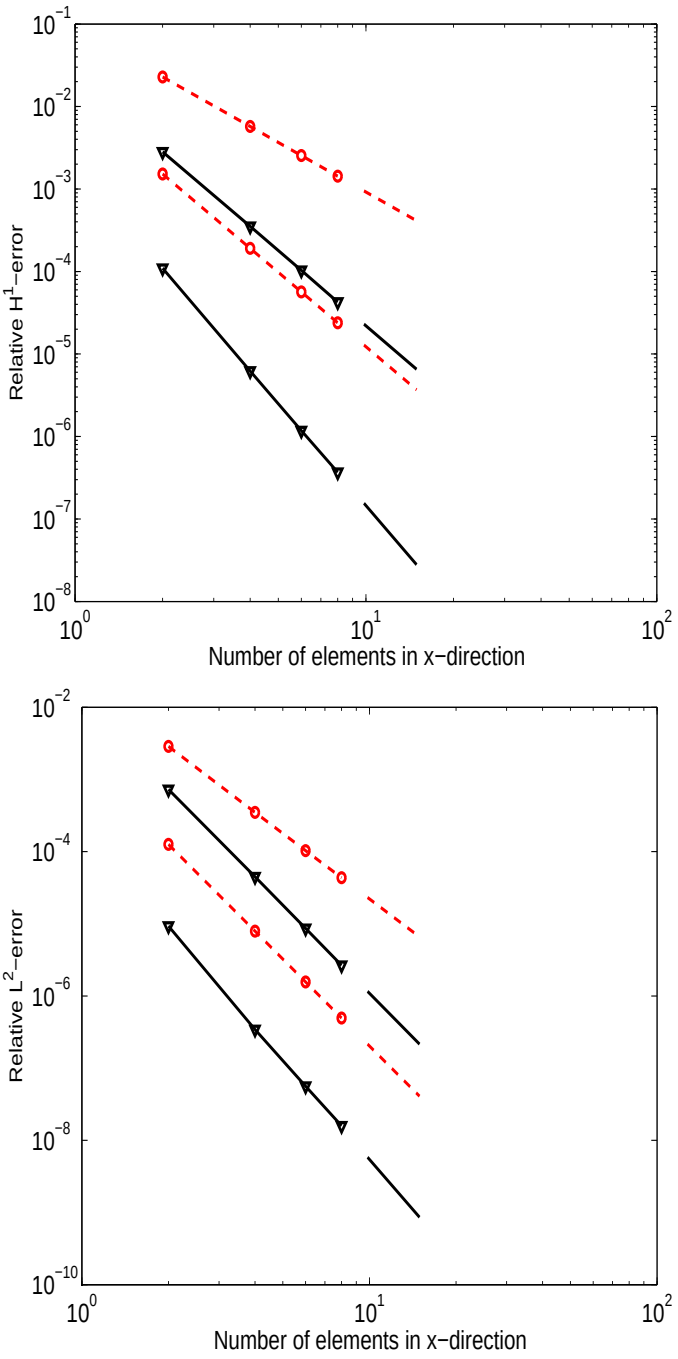

Figure 5: Free edge; Interior region; Uniform mesh; Convergence of the relative H^1- and L^2-errors with $k = 2, 3$ (red dashed line for the original, black solid line for the postprocessed deflection).

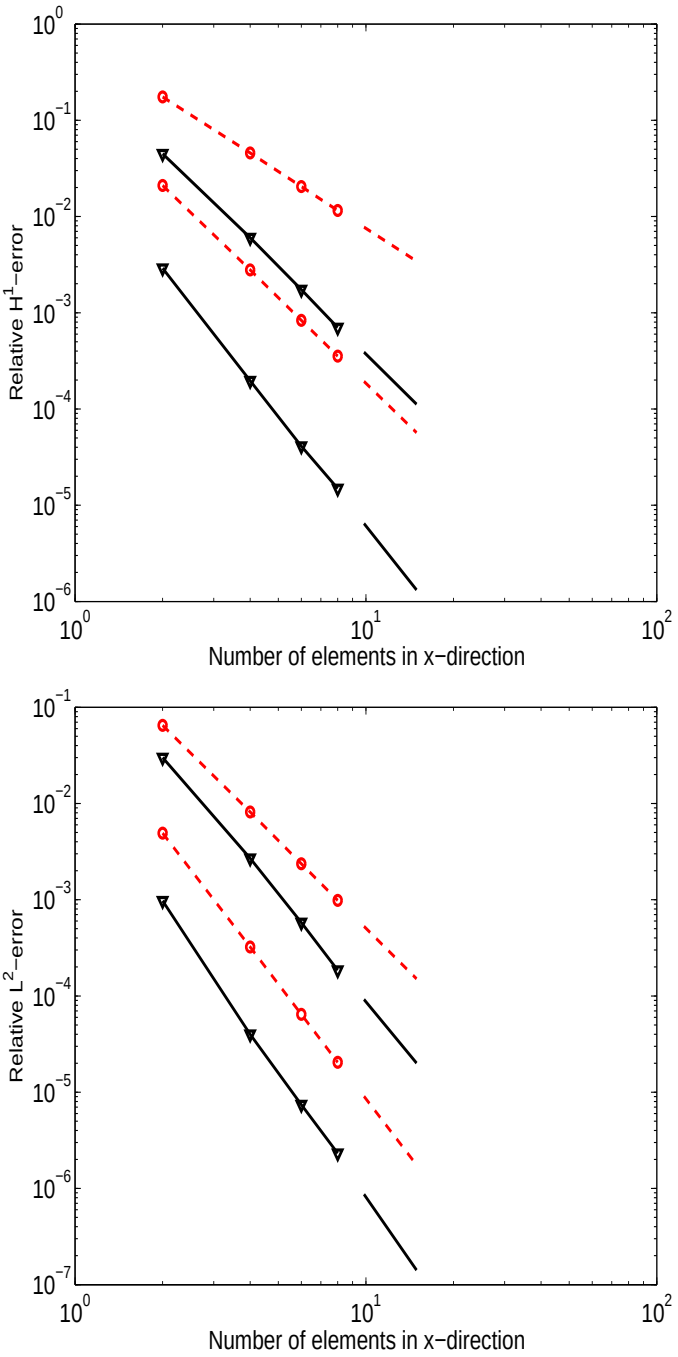

Figure 6: Clamped edge; Boundary region; Uniform mesh; Convergence of the relative H^1- and L^2-errors with $k = 2, 3$ (red dashed line for the original, black solid line for the postprocessed deflection).

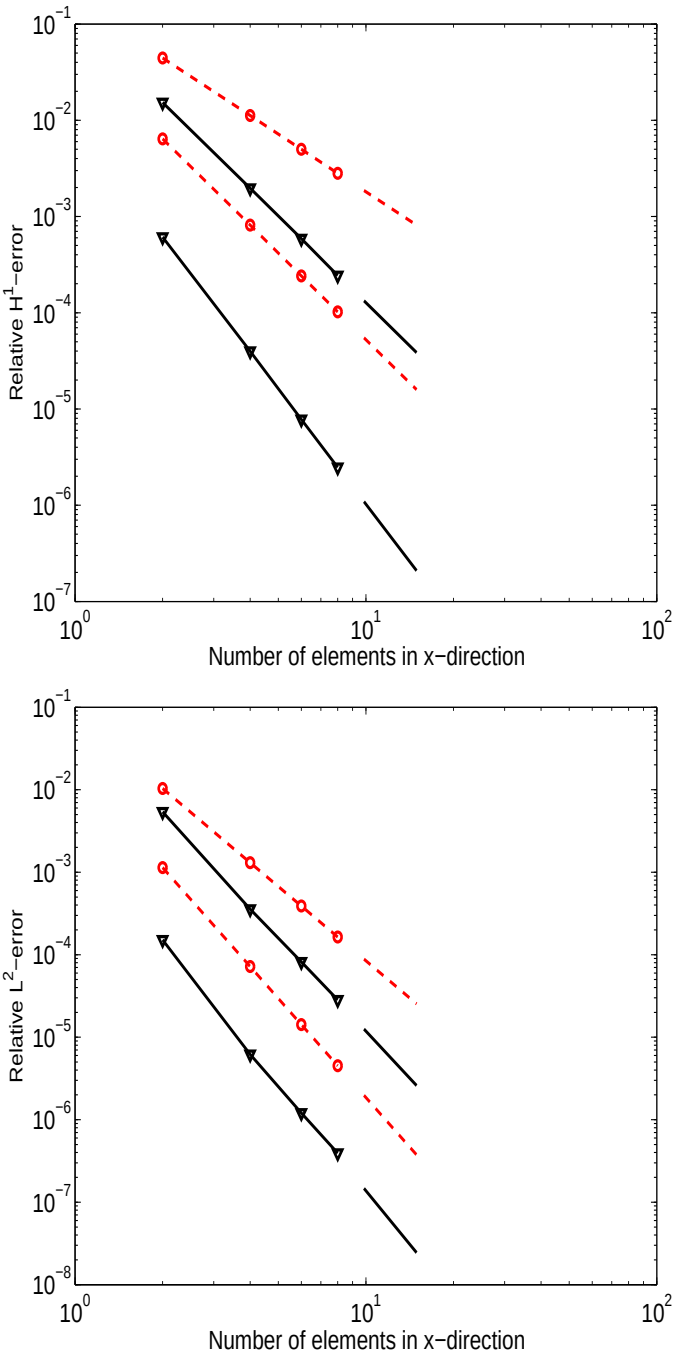

Figure 7: Simply supported edge; Boundary region; Uniform mesh; Convergence of the relative H^1- and L^2-errors with $k = 2, 3$ (red dashed line for the original, black solid line for the postprocessed deflection).

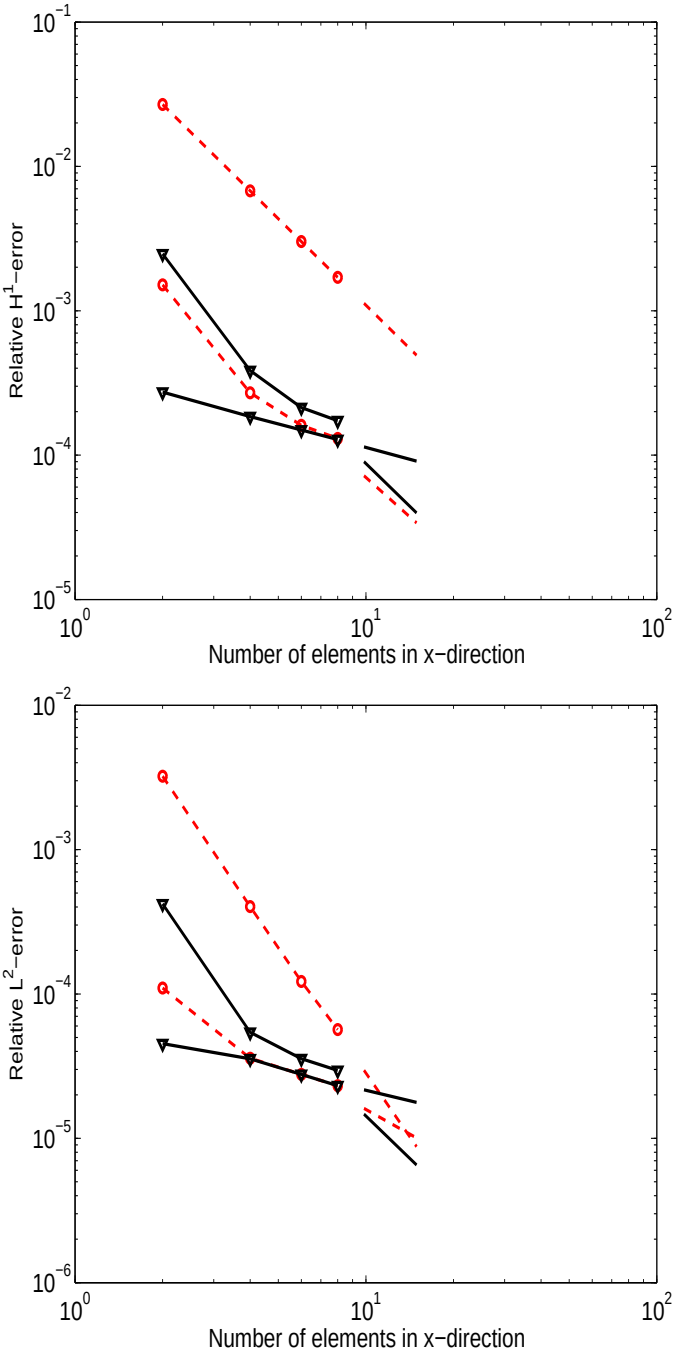

Figure 8: Free edge; Boundary region; Uniform mesh; Convergence of the relative H^1- and L^2-errors with $k = 2, 3$ (red dashed line for the original, black solid line for the postprocessed deflection).

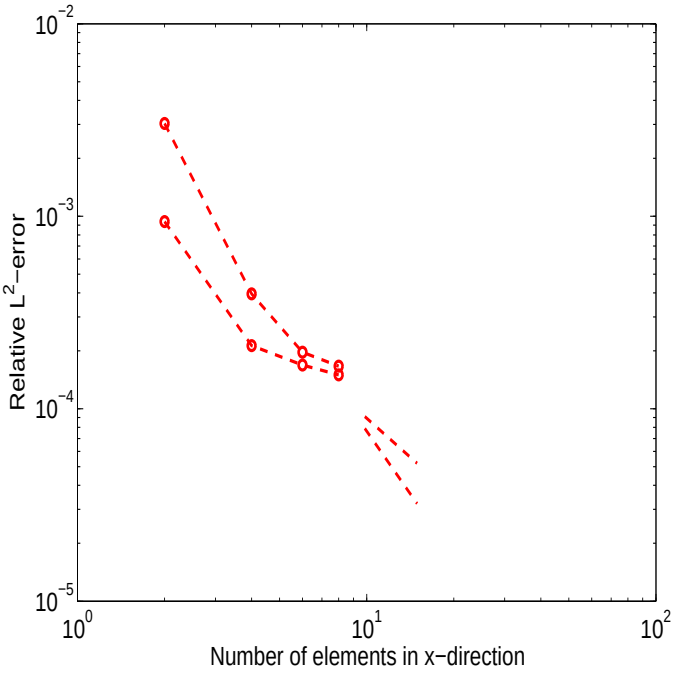

Figure 9: Free edge; Boundary region; Uniform mesh; Convergence of the relative L^2-error for the rotation with $k = 2, 3$.

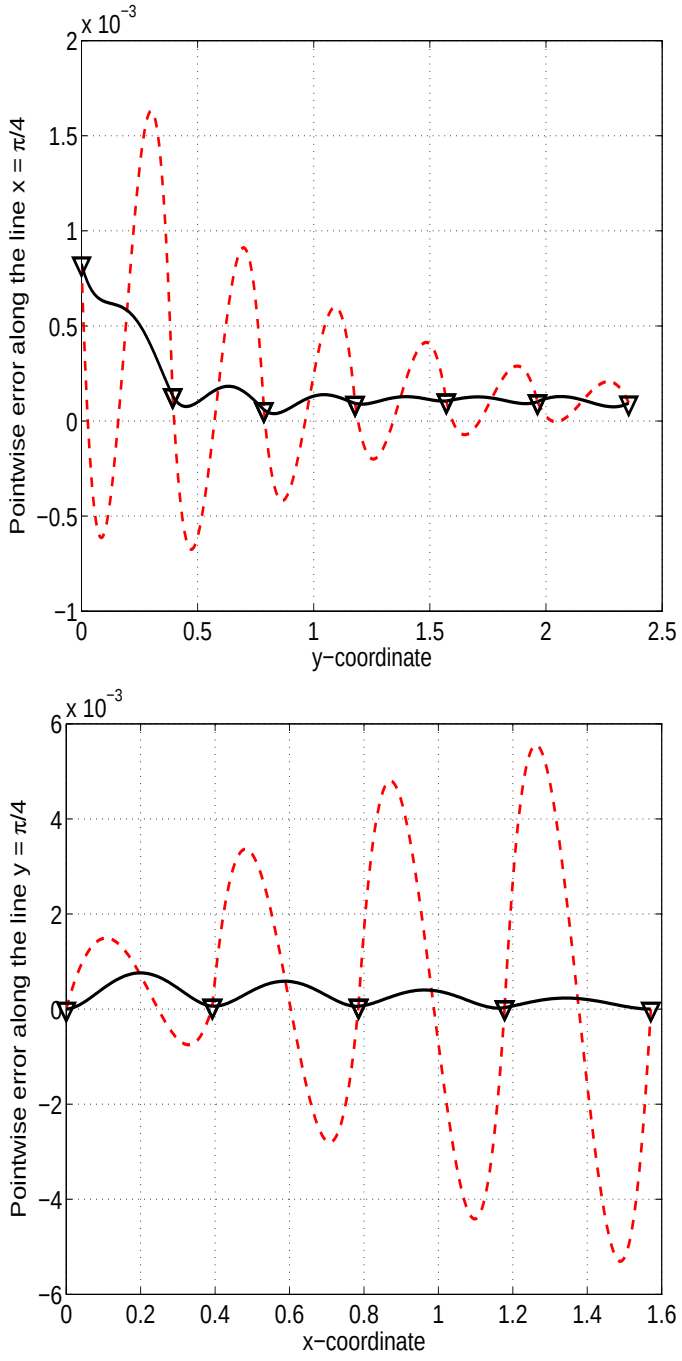

Figure 10: Free edge; Boundary region; Uniform mesh; Pointwise error along the lines $x = \pi/4$ and $y = \pi/4$ for $N = 4$ and $k = 2$ (red dashed line for the original, black solid line for the postprocessed deflection, triangles for vertex values).

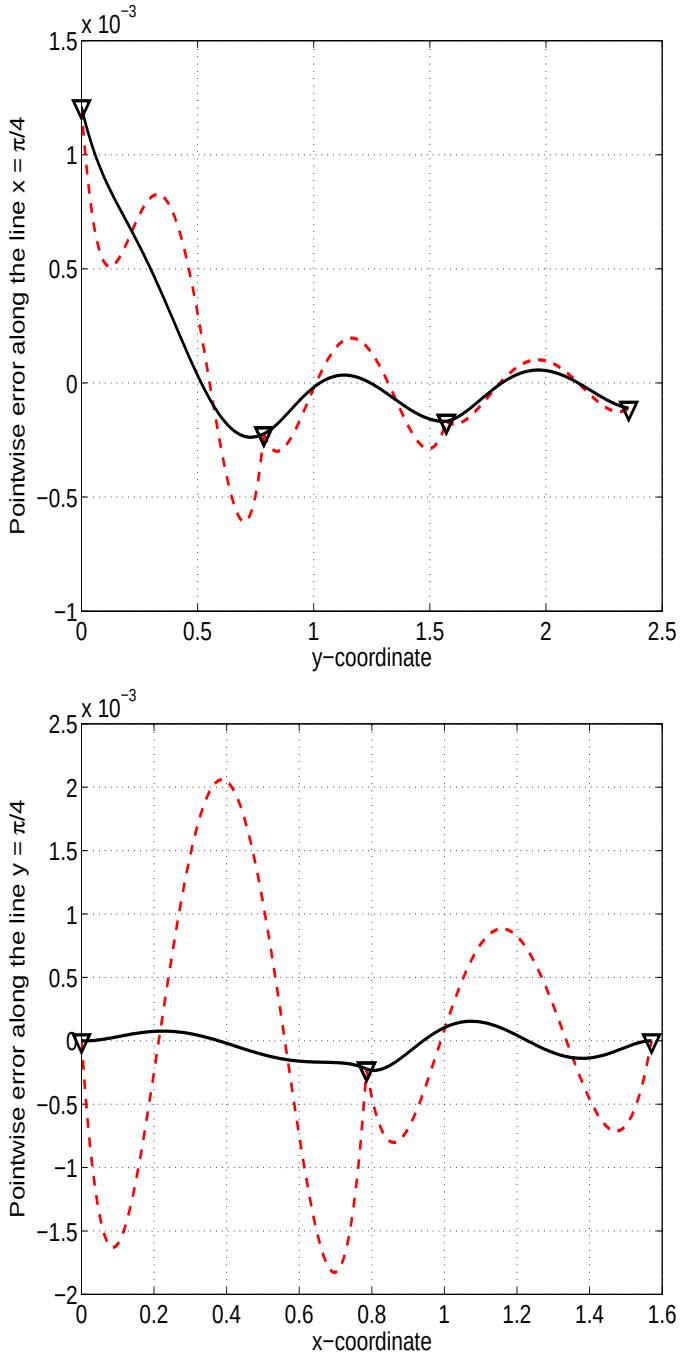

Figure 11: Free edge; Boundary region; Uniform mesh; Pointwise error along the lines $x = \pi/4$ and $y = \pi/4$ for $N = 2$ and $k = 3$ (red dashed line for the original, black solid line for the postprocessed deflection, triangles for vertex values).

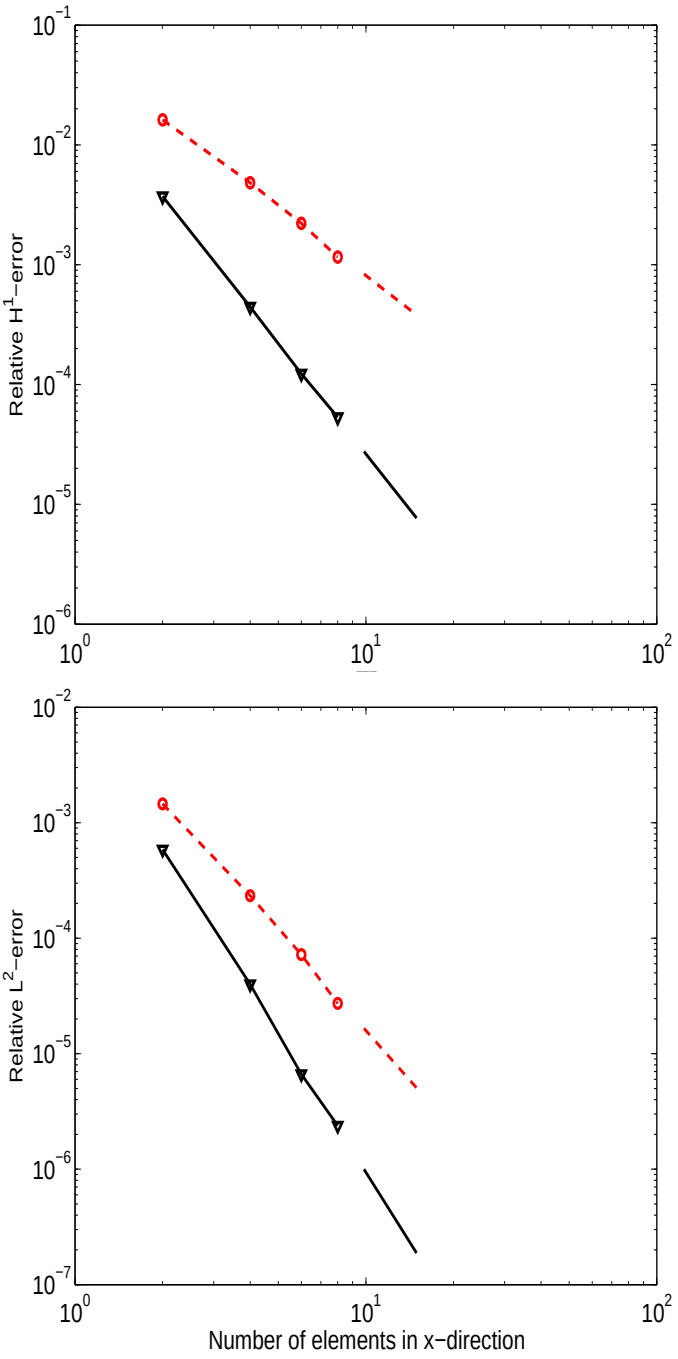

Figure 12: Clamped edge; Non–uniform mesh; Convergence of the relative H^1- and L^2-errors with $k = 2$ (red dashed line for the original, black solid line for the postprocessed deflection).

(continued from the back cover)

A470 Lasse Leskelä
Stabilization of an overloaded queueing network using measurement-based admission control
March 2004

A469 Jarmo Malinen
A remark on the Hille–Yoshida generator theorem
May 2004

A468 Jarmo Malinen , Olavi Nevanlinna , Zhijian Yuan
On a tauberian condition for bounded linear operators
May 2004

A467 Jarmo Malinen , Olavi Nevanlinna , Ville Turunen , Zhijian Yuan
A lower bound for the differences of powers of linear operators
May 2004

A466 Timo Salin
Quenching and blowup for reaction diffusion equations
March 2004

A465 Ville Turunen
Function Hopf algebra and pseudodifferential operators on compact Lie groups
June 2004

A464 Ville Turunen
Sampling at equiangular grids on the 2-sphere and estimates for Sobolev space interpolation
November 2003

A463 Marko Huhtanen , Jan von Pfaler
The real linear eigenvalue problem in C^n
November 2003

A462 Ville Turunen
Pseudodifferential calculus on the 2-sphere
October 2003

HELSINKI UNIVERSITY OF TECHNOLOGY INSTITUTE OF MATHEMATICS
RESEARCH REPORTS

The list of reports is continued inside. Electronical versions of the reports are available at *http://www.math.hut.fi/reports/* .

A477 Tuomo T. Kuusi
Moser's Method for a Nonlinear Parabolic Equation
October 2004

A476 Dario Gasbarra , Esko Valkeila , Lioudmila Vostrikova
Enlargement of filtration and additional information in pricing models: a Bayesian approach
October 2004

A473 Carlo Lovadina , Rolf Stenberg
Energy norm a posteriori error estimates for mixed finite element methods
October 2004

A472 Carlo Lovadina , Rolf Stenberg
A posteriori error analysis of the linked interpolation technique for plate bending problems
September 2004

A471 Nuutti Hyvönen
Diffusive tomography methods: Special boundary conditions and characterization of inclusions
April 2004

ISBN 951-22-7310-1
ISSN 0784-3143